Vol 18 No 10, October 2009
1674-1056/2009/18(10)/4386–07

Chinese Physics B

© 2009 Chin. Phys. Soc.
and IOP Publishing Ltd

Structural phase transition behaviour of Zn_4Sb_3 and its substitutional compounds $(Zn_{0.98}M_{0.02})_4Sb_3$ (M = Al, Ga and In) at low temperatures*

Liu Feng(刘 峰)[a)b)], Qin Xiao-Ying(秦晓英)[a)†], and Liu Mian (刘 冕)[a)]

[a)] *Key Laboratory of Materials Physics, Institute of Solid State Physics, Chinese Academy of Sciences, Hefei* 230031, *China*
[b)] *Department of Applied Mathematics and Physics, Anhui University of Science and Technology, Wuhu* 241000, *China*

(Received 27 April 2008; revised manuscript received 28 April 2009)

Structural phase transitions of Zn_4Sb_3 and its substitutional compounds $(Zn_{0.98}M_{0.02})_4Sb_3$ (M = Al, Ga and In) are investigated by electrical transport measurement and differential scanning calorimetry below room temperature. The results indicate that both $\beta \rightarrow \alpha$ and $\alpha \rightarrow \alpha'$ phase transitions of Zn_4Sb_3 are reversible and exothermic processes, which may be explained as that both the transitions originate from the ordering of the disordered interstitial Zn and vacancies in regular sizes. The derived activation energies of $\beta \rightarrow \alpha$ and $\alpha \rightarrow \alpha'$ phase transition processes for Zn_4Sb_3 are $E_1 = 3.9$ eV and $E_2 = 4.1$ eV, respectively. Although no remarkable influence on activation energy E_2 is observed after Al doping, Al substitution for Zn causes E_1 to increase to 4.6 eV, implying its suppression of $\beta \leftrightarrow \alpha$ transition to a great extent. Moreover, it is found that both $\beta \leftrightarrow \alpha$ and $\alpha \leftrightarrow \alpha'$ transitions are completely prohibited by substitution of either In or Ga for Zn in Zn_4Sb_3. The underlying mechanisms for these phenomena are discussed.

Keywords: Zn_4Sb_3, differential scanning calorimetry, phase transition
PACC: 6150K, 6460

1. Introduction

In the past decade, thermoelectric materials have attracted a great deal of attention for their possible applications in energy conversion and power generation.[1−6] The performance of a thermoelectric material is characterized by a dimensionless figure of merit $ZT(= S^2T/\rho\lambda$, where S, T, ρ and λ denote the Seebeck coefficient (or thermopower), the absolute temperature, the electrical resistivity and the total thermal conductivity, respectively). Recently, semiconducting β-Zn_4Sb_3 has attracted a lot of attention because it has exceptional low thermal conductivity and high thermoelectric properties,[7,8] which possesses largest ZT between 450 K and 670 K among known thermoelectric materials with $ZT = 1.3$ at 670 K.[7] The low thermal conductivity of β-Zn_4Sb_3 is believed to originate from its complex structure.[9,10] The rhombohedral unit cell of β-Zn_4Sb_3 contains three distinct atomic positions (36 Zn, 18 Sb1, and 12 Sb2 in space group $R\bar{3}c$) and can be described as consisting of channels formed by the Zn and Sb1 atoms running along the [001] direction. The channels are centered by chains of Sb2 atoms, which are located on the three-fold axes. Moreover, β-Zn_4Sb_3 manifests the disordering in the framework Zn position, which displays a considerable occupational deficiency (0.89–0.90) and in the occurrence of three weakly occupied (by around 0.06) general positions representing interstitial Zn atoms. The composition obtained from the refined occupancies is $Zn_{3.83}Sb_3$,[9] which accords with experimental results.[7] Figure 1 shows the sketch map of the crystallographic structure of β-Zn_4Sb_3 (based on the data reported in Ref.[9]).

In addition, Zn_4Sb_3 is generally believed to have three modifications, namely α-, β- and γ-Zn_4Sb_3, which are stable below 263 K, between 263 K and 765 K, and above 765 K, respectively.[11,12] The study performed by Nylén *et al* showed that[10] α-Zn_4Sb_3 was an ordered phase with triclinic unit cell (space group $C\bar{1}$) which contains 104 Zn and 80 Sb atoms. Thus, the $\beta \rightarrow \alpha$ phase transition involves in the ordering of Zn interstitial atoms and lattice vacancies

*Project supported by the National Natural Science Foundation of China (Grant No 10774145).
†Corresponding author. E-mail: xyqin@issp.ac.cn

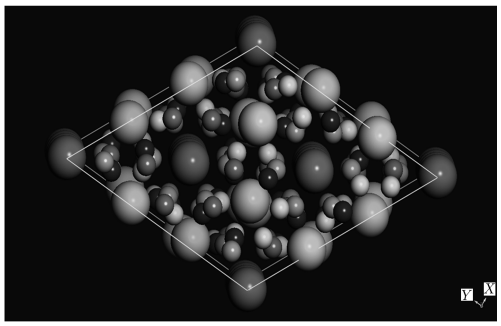


Fig.1. Projection down the c axis of the crystal structure of β-Zn_4Sb_3. Large white and large grey spheres denote 18 Sb1 (18e sites) and 12 Sb2 (12c sites) atoms, respectively. Lattice Zn sites are shown as small black spheres, and three different interstitial sites are represented using small white, greyish and grey spheres, respectively.

at normal Zn sites.[10] Moreover, recent research performed by Nylén *et al*[13] has indicated that apart from the $\beta \rightarrow \alpha$ phase transition at 254 K a second low-temperature $\alpha \rightarrow \alpha'$ phase transition appears below 235 K, and it is found to be related to occupational modulation of slightly Zn deficiency in α phase with respect to $Zn_{13}Sb_{10}$.[13] However, up to now there is very little knowledge of the characteristics of both $\beta \rightarrow \alpha$ and $\alpha \rightarrow \alpha'$ phase transitions and how the doping elements affect the behaviours of both the phase transitions.

On the other hand, it was found that doping in β-Zn_4Sb_3 was very difficult.[14,15] Nakamoto *et al*[16] investigated thermoelectric properties of Cd doped compounds $(Zn_{1-x}Cd_x)_4Sb_3$ and found that its power factor at 300 K took a maximum at a Cd content of 0.2. Meanwhile, their experimental result showed that the $\beta \rightarrow \alpha$ phase transition of Zn_4Sb_3 was not prohibited completely by Cd substitution for Zn. Instead, the anomaly for resistivity and thermopower at the transition was only weakened. To our knowledge, however, there are few studies (other than Cd[16,17]) of the effects of element substitution for Zn on phase transition behaviour of Zn_4Sb_3 below room temperature.

In the present work, β-Zn_4Sb_3 and its substitutional compounds β-$(Zn_{0.98}M_{0.02})_4Sb_3$ (M = Al, Ga and In) were successfully prepared by a melting and hot-pressing method. Their low-temperature phase transition behaviour was investigated by differential scanning calorimetry and electronic transport measurement in a temperature range from 5 K to 310 K. The obtained results were correlated to their structural characteristics.

2. Experimental procedures

Zn_4Sb_3 and $(Zn_{0.98}M_{0.02})_4Sb_3$ (M = Al, Ga and In) compounds used in the present study were synthesized by the melting and hot-pressing method. In this method, the reactions between Sb and molten metals were allowed to take place gradually in evacuated quartz tubes. Appropriate elemental mixtures of Zn(5N) powder, Sb(5N) pieces, M (M = Al, Ga and In)(5N) grains for stoichiometric $(Zn_{1-x}M_x)_4Sb_3$ ($x = 0$ and 0.02) with 1.0 at.% Zn-rich (slight Zn-rich in the mixtures is to compensate for the loss of Zn during preparation) were sealed into evacuated quartz tubes at a pressure of 2×10^{-2} Pa. Then they were heated slowly to 750 °C, and held at this temperature for 12 h. After that the tubes were quickly quenched in water to form $(Zn_{1-x}M_x)_4Sb_3$ ($x = 0$ and 0.02) compounds. The obtained compounds were grinded in agate mortar to fine powders. In order to obtain bulk doped compound $(Zn_{0.98}M_{0.02})_4Sb_3$ (M = Al, Ga and In) samples successfully, hot-pressing was carried out in a furnace equipped with a specially designed WC die and was performed (in vacuum) at relatively low temperature (300 °C) by exerting a high pressure of 600 MPa for 1 h. The obtained bulk samples of 14 mm in diameter and 2–3 mm in thickness, possess good mechanical strength. To measure electrical resistivity, bar-shape specimens of 12 mm×3 mm ×(∼) 2 mm in size were cut from the bulk samples.

The phase structure and compositions of the obtained samples were determined by using x-ray diffraction (XRD). Accurate lattice parameters were measured by XRD with using a Si standard for calibration. DC electrical resistivity was measured in a temperature range from 5 K to 310 K by using the conventional four-probe method. Thermal analysis was conducted at temperatures from room temperature down to 155 K by using Differential Scanning Calorimetry (DSC) (Pyris Diamond DSC, Perkin-Elmer).

3. Results and discussion

3.1. Sample characterization

X-ray diffraction patterns at room temperature for all the samples are shown in Fig.2, where curves (a), (b), (c) and (d) represent the XRD patterns for Zn_4Sb_3, $(Zn_{0.98}Al_{0.02})_4Sb_3$, $(Zn_{0.98}Ga_{0.02})_4Sb_3$ and $(Zn_{0.98}In_{0.02})_4Sb_3$, respectively. It can be seen that single β-phase is obtained for Zn_4Sb_3 and its doped

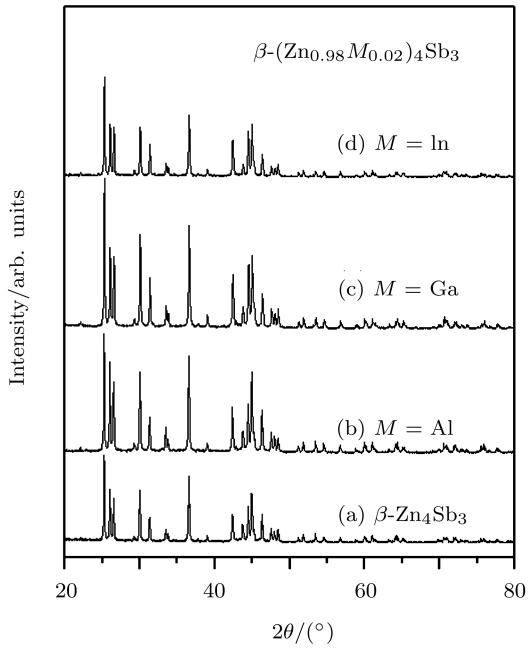


Fig.2. XRD patterns (CuK_α irradiation) of undoped β-Zn_4Sb_3 (a), and M substituted compounds $(Zn_{0.98}M_{0.02})_4Sb_3$ ((b) M = Al, (c) M = Ga, (d) M = In) at 300 K.

compounds with different kinds of dopants and no obvious impurity phase is detectable from the XRD patterns for all compounds. Accurate lattice parameter measurements show that (Fig.3) lattice constants a and c decrease from 12.239 Å and 12.398 Å for β-Zn_4Sb_3 to 12.213 Å and 12.363 Å (1 Å = 0.1 nm) for the Al doped sample, and then changed to 12.218 Å and 12.386 Å for the Ga doped sample, respectively.

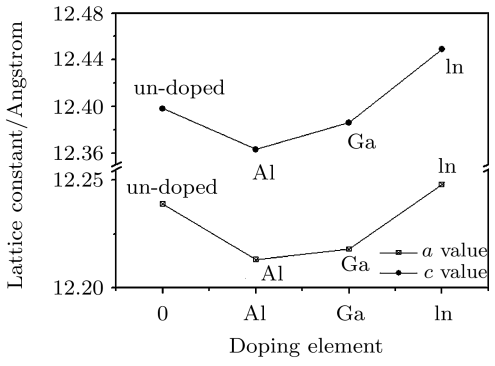


Fig.3. Lattice parameters of β-Zn_4Sb_3 and $(Zn_{0.98}M_{0.02})_4Sb_3$ (M = Al, Ga and In) at 300 K.

However, lattice constants a and c increase respectively to 12.248 Å and 12.449 Å after doping In. The present result indicates, on the one hand, that Al, Ga and In were successfully substituted for Zn in Zn_4Sb_3, forming doped compounds $(Zn_{0.98}M_{0.02})_4Sb_3$ (M = Al, Ga and In), and, on the other hand, that the doped elements M would display high ionicity mainly with trivalence, for ionic radius of Zn^{2+} (0.74 Å) is larger than those of Al^{3+} (0.51 Å) and Ga^{3+} (0.62 Å), but smaller than that of In^{3+} (0.81 Å).

3.2. Structural phase transition

The curves for DC electrical resistivity versus temperature for Zn_4Sb_3 and $(Zn_{0.98}M_{0.02})_4Sb_3$ (M = Al, Ga and In) in a range of 5–310 K are presented in Fig.4. One can see that the temperature dependence of the resistivity for Zn_4Sb_3 shows basically metallic-like (i.e., $d\rho/dT > 0$) behaviour in the whole temperature range measured. The observed anomaly in the ρ–T curve between 265 K and 230 K is associated with the structural transition from β to α/α'-phase:[16,18,19] the transition (peak) temperature T_S observed here is around 253 K, which is lower than 263 K reported by Mayer *et al*[11] and Tapiero *et al*,[12] but higher than that reported by Nakamoto *et al*.[16] In the case of $(Zn_{0.98}Al_{0.02})_4Sb_3$ (Fig.4(b)), the temperature dependence of ρ is similar to that for pure Zn_4Sb_3. However, as compared with that of Zn_4Sb_3, the anomaly caused by the phase transition (the height of the peak) reduces substantially (see Fig.4 and the inset), thereby suggesting that Al substitution for Zn can suppress the transition to a certain degree. In addtion, Al doping is found to cause the transition (peak) temperature of $\beta \rightarrow \alpha/\alpha'$-phase to shift from 253 K to 246 K, but the end temperature seems to be unchanged obviously (remaining about 235 K). In contrast to Al doping, the

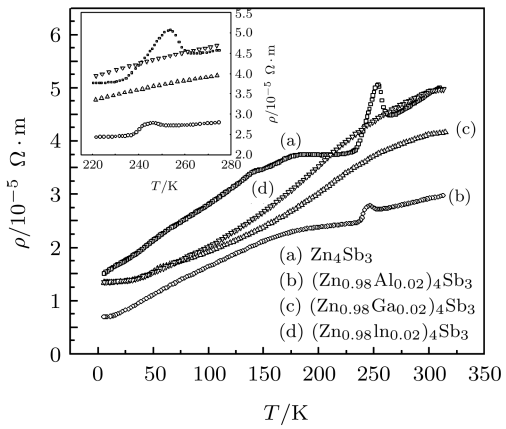


Fig.4. The temperature dependence of the electrical resistivity for Zn_4Sb_3 (a), $(Zn_{0.98}Al_{0.02})_4Sb_3$ (b), $(Zn_{0.98}Ga_{0.02})_4Sb_3$ (c) and $(Zn_{0.98}In_{0.02})_4Sb_3$ (d). Inset shows the magnified plots in temperature range 220 K to 275 K.

electrical resistivity ρ of $(Zn_{0.98}M_{0.02})_4Sb_3$ (M = Ga and In) decreases monotonically with temperature de-

creasing in the whole measured temperature range (from 5 K to 310 K), and no such anomaly in the ρ–T curves is detected (see the inset of Fig.4). This result suggests that the $\beta \rightarrow \alpha/\alpha'$ phase transition is fully prohibited by substituting either Ga or In for Zn.

In order to examine the $\beta \leftrightarrow \alpha/\alpha'$ phase transition behaviour of Zn_4Sb_3 system in more detail, low-temperature DSC analyses were carried out. Figure 5 gives the DSC curves for Zn_4Sb_3 and $(Zn_{0.98}M_{0.02})_4Sb_3$ (M = Al, Ga and In) samples. From the DSC curve of Zn_4Sb_3 (curve (a) in Fig.5) one can see that during cooling a large exothermal peak P_1 is located in an interval of 265–240 K and a smaller exothermal peak P_2 occurs in an interval of 240–233 K, which indicates that the corresponding anomaly appearing in the plots of ρ–T in Fig.4 is actually composed of two sub-transitions. The present result is consistent with the previous results reported by other researchers,[13] i.e. the large peak P_1 corresponds to $\beta \rightarrow \alpha$ phase transition and the smaller peak P_2 at lower temperatures corresponds to $\alpha \rightarrow \alpha'$ phase transition.

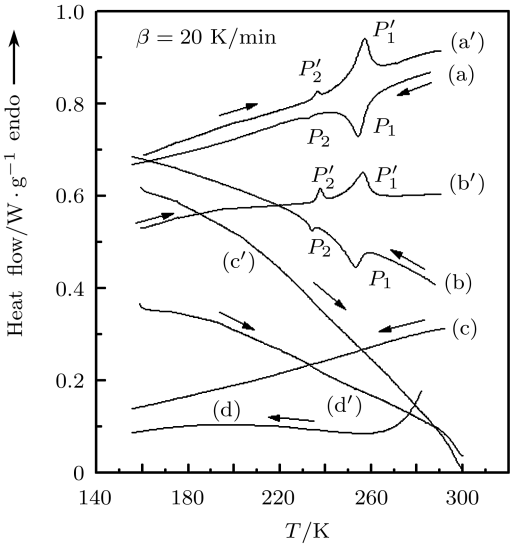


Fig.5. DSC curves for Zn_4Sb_3 (a), $(Zn_{0.98}Al_{0.02})_4Sb_3$ (b), $(Zn_{0.98}Ga_{0.02})_4Sb_3$ (c) and $(Zn_{0.98}In_{0.02})_4Sb_3$ (d) during cooling scan. (a′), (b′), (c′) and (d′) show their corresponding DSC curves in heating process.

To examine the characteristics of the phase transitions and doping effects on the transitions, DSC analyses with different scanning rates (during heating) were performed for Zn_4Sb_3 and $(Zn_{0.98}Al_{0.02})_4Sb_3$ as shown in Figs.6(a) and 6(b), respectively. It can be seen that

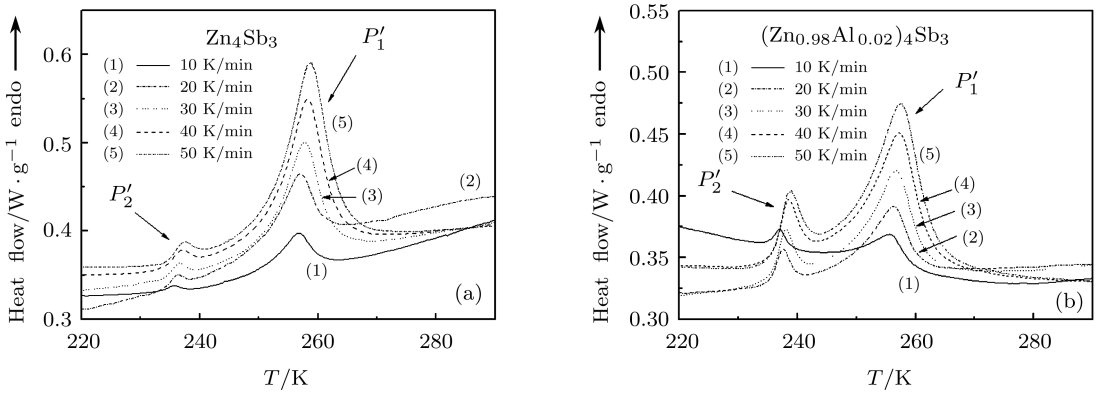


Fig.6. Endothermal curves of DSC for Zn_4Sb_3 (a) and $(Zn_{0.98}Al_{0.02})_4Sb_3$(b) at five different heating rates (10, 20, 30, 40 and 50 K · min^{-1}).

for both the samples the heights of endothermal peaks P_1' and P_2' increase and the positions of the peaks shift toward higher temperatures when the scanning rate increases. The enthalpy changes ΔH_1 and ΔH_2 are shown in Fig.7: ΔH_1 and ΔH_2 do not change obviously with scanning rate or heating-cooling circle, indicating their reversibility. The smaller value for ΔH_1 at scanning rate 10 K/min may result from measurement error of ΔH_1 due to smaller peak height in slow scanning. Averagely, ΔH_1 = 1.95 J/g (or 1209 J/mol that is calculated from its chemical formula, $Zn_{3.9}Sb_3$.[9,13]) that is about 28 times greater

than ΔH_2 (7.0×10^{-2} J/g, or 43 J/mol). During cooling, correspondingly two exothermic peaks P_1 and P_2 with almost the same enthalpy change as those for P_1' and P_2' appear in the DSC curves (curve (a) in Fig.5), indicating further that both the transitions are reversible. Obviously, the appearance of endothermic peaks P_1' and P_2' indicates that both $\alpha' \rightarrow \alpha$ and $\alpha \rightarrow \beta$ phase transitions are endothermic processes (curve (a′) in Fig.5). In addition, the fact that both $\beta \rightarrow \alpha$ transition and $\alpha \rightarrow \alpha'$ phase transition are exothermal process indicates that the assembly changes consecutively to lower energetic states, which is in agreement with ordering processes of the interstitial Zn atoms (and vacancies) in β-Zn_4Sb_3 during these transitions.[10,13]

On the other hand, after doping either Ga or In the two exothermal (endothermic) peaks P_1 (P_1') and P_2 (P_2') disappear in DSC curves during cooling (heating) scan (curves (c) and (d) in Fig.5), indicating once more that both $\beta \leftrightarrow \alpha$ and $\alpha \leftrightarrow \alpha'$ phase transitions have been prohibited completely by substituting either Ga or In for Zn in Zn_4Sb_3, which is in agreement with the measurements of the resistivity. In contrast, after doping Al the two exothermal peaks are still existent and reversible (curves (b) and (b′) in Fig.5.). However, an obvious difference is that the onset temperatures T_{o1} and T_{o2} for the two transition peaks P_1 and P_2 change from 259 K and 234 K to 257 K and 236 K, respectively as shown in Table 1. Moreover, it is found that after Al doping, ΔH_1 decreases from about 1.95 J/g (1209 J/mol) to 1.20 J/g (745 J/mol); while ΔH_2 increases from 0.07 J/g (43 J/mol) to 0.22 J/g (136 $J \cdot mol^{-1}$). However, the total enthalpy change ($\Delta H_1 + \Delta H_2$) for Zn_4Sb_3 is larger than that of $(Zn_{0.98}Al_{0.02})_4Sb_3$, thereby indicating that the substitution of Al for Zn enhances the stability of β phase.

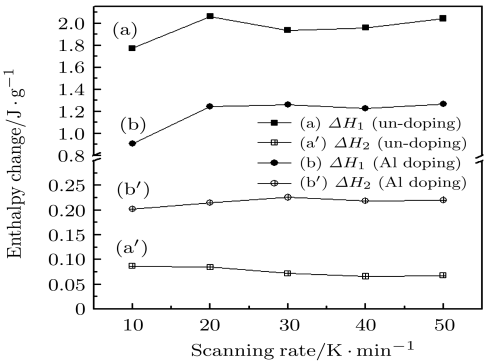


Fig.7. Enthalpy change ΔH_1 of $\beta \rightarrow \alpha$ phase transition and ΔH_2 of $\alpha \rightarrow \alpha'$ phase transition for Zn_4Sb_3 ((a) and (a′)) and $(Zn_{0.98}Al_{0.02})_4Sb_3$((b) and (b′)) each as a function of scanning rate performed consecutively.

Table 1. Onset temperatures T_{o1} and T_{o2}, enthalpy changes ΔH_1 and ΔH_2, and apparent activation energies E_1 and E_2 of the endothermic processes corresponding to P_1 and P_2 peaks, respectively, in the DSC curves for Zn_4Sb_3 and $(Zn_{0.98}Al_{0.02})_4Sb_3$.

	T_{o1}/K	T_{o2}/K	ΔH_1/J · mol^{-1}	ΔH_2/J · mol^{-1}	E_1/eV	E_2/eV
Zn_4Sb_3	259	234	1209±15	43±10	3.9±0.7	4.1±0.6
$(Zn_{0.98}Al_{0.02})_4Sb_3$	257	236	745±15	136±10	4.6±0.7	4.0±0.5

As mentioned above, the positions of the peaks shift toward higher temperatures when the (heating) scanning rate increases. The variation of the endothermal peak with heat scanning rate can be analysed by using Kissinger equation:[20]

$$\ln\left\{\frac{\beta}{T_{\max}^2}\right\} = \ln\left\{\frac{RA}{E}\right\} - \frac{E}{R}\frac{1}{T_{\max}}\ , \tag{1}$$

where β is the heating rate in DSC scanning, $T_{\max}$ the peak temperatures of endothermal P_1' and P_2', E the apparent activation energy, A the frequency coefficient, and R the gas constant. Figure 8 shows the plots of $\ln(\beta/T_{\max}^2)$ vs. $1/T_{\max}$. By best (linear) fitting the experimental data to formula (1), one can obtain apparent activation energies E_1 and E_2 corresponding to $\beta \leftrightarrow \alpha$ and $\alpha \leftrightarrow \alpha'$ phase transitions for Zn_4Sb_3, which are 3.9 eV and 4.1 eV, respectively as listed in Table 1. Both of the activation energies E_1 (3.9 eV) and E_2 (4.1 eV) obtained here for Zn_4Sb_3 are comparable to the activation energy (5.3 eV) for the structural transition corresponding to an order–disorder change in oxygen ion arrangement in $La_2Mo_2O_9$.[21] Al doping makes E_1 increase from 3.9 eV to 4.6 eV, demonstrating that Al substitution adds resistance to the $\beta \leftrightarrow \alpha$ phase transition although Al doping cannot prohibit its occurrence. E_2 (4.0 eV) for $(Zn_{0.98}Al_{0.02})_4Sb_3$ is similar to that for Zn_4Sb_3 within experimental errors, which implies that influence of Al doping on $\alpha \leftrightarrow \alpha'$ transition is not remarkable.

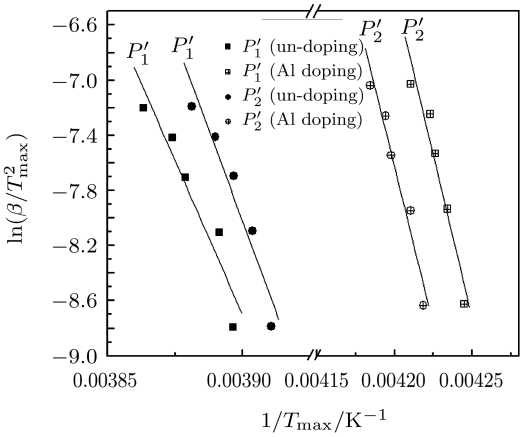


Fig.8. Kissinger plots of the peaks P_1' and P_2' for the $\beta \rightarrow \alpha$ and $\alpha \rightarrow \alpha'$ phase transitions of Zn_4Sb_3 and $(Zn_{0.98}Al_{0.02})_4Sb_3$ respectively.

The above results indicate that the $\beta \leftrightarrow \alpha$ and $\alpha \leftrightarrow \alpha'$ phase transitions are fully prohibited by the substitution of either Ga or In for Zn, while Al doping cannot effectively impede the occurrence of the phase transitions. One possible explanation of this difference among In, Ga and Al would be related to their different atomic (ionic) radii. Since there is relationship where radius R_{In} (for In^{3+}) > R_{Ga} (for Ga^{3+}) > R_{Al} (for Al^{3+}), the dopant with larger radius should have a stronger inhibition effect on the phase transitions. Nevertheless, the prohibition of the phase transitions by the substitution of either Ga or In for Zn cannot be fully and reasonably explained by the larger ionic radii of Ga^{3+} and In^{3+}, for the experiments of Nakamoto *et al*[16] showed that the Cd substitution for Zn could not prohibit effectively the $\beta \rightarrow \alpha$ phase transition of Zn_4Sb_3, though ionic radius of Cd^{2+} (0.97 Å) is larger than that of Zn^{2+} (and even larger than radius of In^{3+}). An alternative interpretation to this phenomenon may consist in the possibility that Cd and M (= In, Ga and Al) occupy (dominantly) different kinds of Zn sites. According to the previous investigations,[13,22] the structures of both β-Zn_4Sb_3 and α-Zn_4Sb_3 are composed of the same building units, i.e. Zn_2Sb_2 planar rhomboids. In β-Zn_4Sb_3, Zn_2Sb_2 rhomboid forms chains by sharing common Sb1 atoms. These chains run in three different directions in the rhombohedral structure and result in a framework with channels along the c direction, which are centred by Sb2 atoms. By Comparing changes of Zn_2Sb_2 rhomboids in both structures, they found that twenty-one out of the 26 Zn positions in α-Zn_4Sb_3 corresponded to regular framework Zn atoms within the rhomboid rings in β-Zn_4Sb_3. The remaining five "non-rhombohedral" Zn atoms are then associated with the interstitial Zn atoms in disordered β-Zn_4Sb_3. These atoms are assembled in clusters consisting of a triangle with a tail of two more Zn atoms attached. Two five-atom clusters are grouped together and related to each other by a centre of inversion. Each pair of five-atom clusters corresponds to three pairs of Zn atoms from the regular rhomboid ring framework in β-Zn_4Sb_3. These missing pairs of Zn atoms are associated with the vacancies in β-Zn_4Sb_3. Therefore, any factors that perturb Zn interstitial positions and/or vacancies (in normal lattice) will interfere with the $\beta \rightarrow \alpha$ phase transition. Hence, it is conceivable that dopant atoms that replace Zn (i.e. one of the five atoms in the clusters) at interstitial sites or normal Zn in the vicinity of the (Zn) lattice vacancies will have much stronger effect on the $\beta \rightarrow \alpha$ phase transition than those replacing Zn in normal lattice far from Zn vacancies (or interstitial Zn clusters). In other words, if dopant atoms replace Zn atoms mainly at interstitial sites or nearby normal sites, it will have a direct or strong resistance against motion and a diffusion of the (other) interstitial Zn atoms and vacancies to form five-atom clusters, thus impeding the $\beta \rightarrow \alpha$ phase transition severely, which would be the case for the substitution of In or Ga for Zn. However, since the radius of Al^{3+} (0.51 Å) is much (∼69%) smaller than that of Zn^{2+} (0.74 Å), the resistance of the doped Al atoms (ions) to the diffusions of interstitial Zn atoms and vacancies would be not enough to prohibit its occurrence no matter where it is in the lattice of β-Zn_4Sb_3, but only add some difficulties to the diffusion of the interstitial Zn atoms and vacancies, as manifested by the increase of activation energy E_1 after Al doping (Table 1).

4. Conclusions

Structural phase transitions of Zn_4Sb_3 and $(Zn_{0.98}M_{0.02})_4Sb_3$ (M = Al, Ga and In) are investigated at low temperatures. The results indicate that both $\beta \rightarrow \alpha$ and $\alpha \rightarrow \alpha'$ phase transitions of Zn_4Sb_3 are exothermic (corresponding enthalpy change $\Delta H_1 = 1209\ J \cdot mol^{-1}$ and $\Delta H_2 = 43\ J \cdot mol^{-1}$, respectively,) and reversible processes, verifying that both transitions originate from the ordering of the disordered interstitial Zn atoms. The obtained high activation energies ($E_1 = 3.9$ eV and $E_2 = 4.1$ eV, respectively) for both transitions are believed to be related to its complex hexagonal rhombo-

hedric structure of β-Zn_4Sb_3. Moreover, both $\beta \leftrightarrow \alpha$ and $\alpha \leftrightarrow \alpha'$ transitions are found to be completely prohibited by doping either In or Ga into Zn_4Sb_3. Besides, the experimental results reveal that the Al doping cannot fully prohibit the phase transitions, and only suppress the $\beta \leftrightarrow \alpha$ transition as evidenced by the increase of the activation energy E_1 and the reduction of corresponding enthalpy change ΔH_1.

References

[1] Disalvo F J 1999 *Science* **285** 703

[2] Venkatasubramanian R, Siivola E, Colpitts T and Quinn B O 2001 *Nature* **413** 597

[3] Mahan G, Sales B and Sharp J 1997 *Physics Today* **50** 42

[4] Li H, Tang X F, Liu T X, Song C and Zhang Q J 2005 *Acta Phys. Sin.* **54** 5481 (in Chinese)

[5] Tritt T M 1999 *Science* **283** 804

[6] Zhu T J, Zhao X B, Yan M, Hu S H, Li T and Zhou B C 2000 *Materials Letters* **46** 44

[7] Caillat T, Fleurial J P and Borshevsky A 1997 *J. Phys. Chem. Solids* **58** 1119

[8] Qi Q, Tang X F, Xiong C, Zhao W Y and Zhang Q J 2006 *Acta Phys. Sin.* **55** 5539 (in Chinese)

[9] Snyder G J, Christensen M, Nishibori E, Caillat T and Iversen B B 2004 *Nat. Mater.* **3** 458

[10] Nylén J, Andersson M, Lidin S and Häussermann U 2004 *J. Am. Chem. Soc.* **126** 16306

[11] Mayer H W, Mikhail I and Schubert K 1978 *J. Less Common Met.* **59** 43

[12] Tapiero M, Tarabichi S, Gies J G, Noguet C, Zielinger J P, Joucla M, Loison J and Robino M 1985 *Solar Energy Materials* **12** 257

[13] Nylén J, Lidin S, Andersson M, Iversen B B, Liu H, Newman N and Häussermann U 2007 *Chem. Mater.* **19** 834

[14] Koyanagi T, Hino K, Nagamoto Y, Yoshitake H and Kishimoto K 1997 *Proc. 16th International Conference on Thermoelectrics* p463

[15] Tsutsui M, Zhang L T, Ito K and Yamaguchi M 2004 *Intermetallics* **12** 809

[16] Nakamoto G, Souma T, Yamaba M and Kurisu M 2004 *J. Alloys Compd.* **377** 59

[17] Liu F, Qin X Y and Li D 2007 *J. Phys.* D: *Appl. Phys.* **40** 4974

[18] Souma T, Nakamoto G and Kurisu M 2001 *Proc. 20th International Conference on Thermoelectrics* p274

[19] Souma T, Nakamoto G and Kurisu M 2002 *J. Alloys Compd.* **340** 275

[20] Kissinger H E 1957 *Anal. Chem.* **29** 1702

[21] Wang X P and Fang Q F 2001 *J. Phys: Condens. Matter* **13** 1641

[22] Mikhaylushkin A S, Nylén J and Häussermann U 2005 *Chem. Eur. J.* **11** 4912